# An approach for quasi-continuous time-lapse seismic monitoring with sparse data

*Adeyemi Arogunmati* and Jerry M. Harris, Stanford University, California, USA*

**Summary**

An approach for quasi-continuous, geophysical time-lapse monitoring with sparse seismic data is proposed. This approach takes advantage of the small changes in the seismic property of a geological reservoir that are expected to occur in a small time interval. The goal of this approach is to obtain high temporal and spatial resolution in reconstructed, time-lapse geophysical images using comparable resources that would have provided high spatial but low temporal resolution images with conventional approaches. This is done by acquiring spatially sparse data at small time intervals. In this case, a spatially sparse dataset refers to that dataset which is a small fraction (as little as 5%) of what would be acquired to reconstruct a high spatial resolution tomographic image of the subsurface. The high spatial resolution obtained by the proposed approach occurs because unrecorded data are predicted from future and past data. With high temporal and spatial resolution, early detection of important reservoir changes is more likely to occur.

**Introduction**

Geophysical imaging has played a large part in subsurface monitoring projects, especially in petroleum reservoir monitoring projects (e.g., Harris et al., 1995; Rickett and Lumley, 2001). This is primarily due to the kind of seismic changes that occur in the reservoir rock properties (Wynn, 2003). In addition, seismic data analysis is a well developed and understood subject (Yilmaz, 1987; Yilmaz, 2001). Seismic signals are able to penetrate deep into the earth and can be used in virtually any geologic setting (Wynn, 2003). The use of seismic tomography in time-lapse monitoring takes advantage of the changes in a seismic property of the reservoir rock during the time interval under consideration. For example, a reservoir velocity model can be quantitatively reconstructed from either seismic reflection or transmission traveltimes using tomography.

Consider a time-lapse seismic monitoring study designed to last for several decades as might be the case in whole-life monitoring of a petroleum reservoir or for a $CO_2$ storage site. The conventional approach to monitoring is to acquire a large amount of seismic data such that a high spatial resolution image of the subsurface can be obtained each time a dataset is acquired. The time intervals between successive data acquisition campaigns are often so large that there are large changes in the successive seismic data acquired. The time intervals are usually of the order of years (e.g., Mathisen et al., 1995; Landrø et al., 1999; Arts et al., 2004). Such a strategy works very well for some time-lapse projects but for other applications such as monitoring $CO_2$ storage, the late identification of a reservoir leak by a year could have dire consequences. In other words, some time-lapse monitoring strategies are more effective when the changes in successive time-lapse datasets are small. In such cases, temporal resolution is as important as spatial resolution, and sometimes, more important.

If resources are to be kept comparable, two scenarios are possible – acquiring data such that the monitoring provides either high spatial resolution and low temporal resolution images, or low spatial resolution and high temporal resolution. In the second scenario, low spatial resolution results because a small amount of data is acquired each time, and high temporal resolution results because data are acquired more frequently. The traditional approach to inverting sparse data is to reduce the number of model parameters solved. Because only a fraction of the data that will normally be used to get a high resolution image is used, the resulting seismic image has a lower spatial resolution. We propose to estimate unrecorded data (Harris et al., 2004; 2007; 2008), and then reconstruct geophysical models without reducing the number of model parameters solved, thereby maintaining the high spatial resolution.

Although the idea posed here is somewhat similar to the recently developed concept of compressive sampling (Candès and Romberg, 2007) in the sense that sparse data are acquired and used in estimating unrecorded data, we deal here with datasets that are even more sparse than what would be acquired as compressive sampling. Also, we take advantage of the large portion of the data space available in the dense baseline data.

**Theory**

Let the dense time-lapse data be composed of a recorded sparse part and an unrecorded part. i.e.

$$\mathbf{d}_d = \mathbf{S}\mathbf{d}_d + (\mathbf{I} - \mathbf{S})\,\mathbf{d}_d \qquad (1)$$

$$\mathbf{d}_d = \mathbf{d}_s + \mathbf{d}_u \qquad (2)$$

where $\mathbf{S}$ is the data sampling operator that selects which data are recorded from the “dense” dataset $\mathbf{d}_d$, and $\mathbf{d}_s$ and $\mathbf{d}_u$ are “sparse” and “unrecorded” datasets respectively.

From (1) and (2), we see that

$$\mathbf{d}_s = \mathbf{S}\mathbf{d}_d \;;\quad \mathbf{d}_u = (\mathbf{I} - \mathbf{S})\,\mathbf{d}_d \qquad (3)$$

In this notation, each vector $\mathbf{d}$ contains all previously measured and future measured data. Our goal is to estimate the unrecorded dataset, $\mathbf{d}_u$. Here, $\tilde{\mathbf{d}}_u$ is the model (unrecorded data) estimated from data $\mathbf{d}_s$. The fitting goal for estimating $\mathbf{d}_u$ is

$$\mathbf{A}\mathbf{d}_d \approx \mathbf{0} \qquad (4)$$

where the operator, **A** is the model constraint operator, or estimation operator. If we assume the estimated data $\tilde{\mathbf{d}}_d$ is approximately the dense data $\mathbf{d}_d$, equation (4) can be re-written as

$$\mathbf{A}\tilde{\mathbf{d}}_d \approx \mathbf{0} \qquad (5)$$

which gives

$$\mathbf{A}\mathbf{d}_s + \mathbf{A}\tilde{\mathbf{d}}_u \approx \mathbf{0} \qquad (6)$$

The estimated unrecorded data, $\tilde{\mathbf{d}}_u$ is then obtained using (6), and minimizing the objective function

$$\Phi = \left\| \mathbf{A}\tilde{\mathbf{d}}_u + \mathbf{A}\mathbf{d}_s \right\|^2 \qquad (7)$$

**Time-lapse Field Monitoring Example**

The field data example presented here are crosswell data from the McElroy field in West Texas. The datasets were acquired to monitor velocity changes in the reservoir in response to $CO_2$ injection (Harris et al., 1995; Lazaratos and Marion, 1997) between 1993 and 1995. The wells are over 3000ft deep and are separated by approximately 600ft. Figure 1 shows common-shot gathers data from the surveys. First arrival seismic traveltimes were picked from the data. The largest traveltime differences occur at the depths corresponding to the location of the reservoir between 2750 and 3150 ft. Using these traveltimes, velocity models were reconstructed using the tomography code, FAST (Zelt and Barton, 1998). Figure 2 shows the reconstructed velocity models and the difference between them when the complete dataset in both cases are used. The most obvious difference in the velocity models is the significant drop in the p-wave velocity between 1993 and 1995, resulting from the injection of $CO_2$ into the reservoir.

Having a time interval of two years between the baseline image and the monitor image is satisfactory for some monitoring projects. However, if potentially dangerous consequences could occur from an abnormality in the reservoir, it will be necessary to monitor the reservoir with a finer sampling in time. Also, if resources necessary for data acquisition are limited, a more efficient time-lapse monitoring strategy is needed. This, scenario illustrates the need for a quasi-continuous monitoring strategy using sparse data.

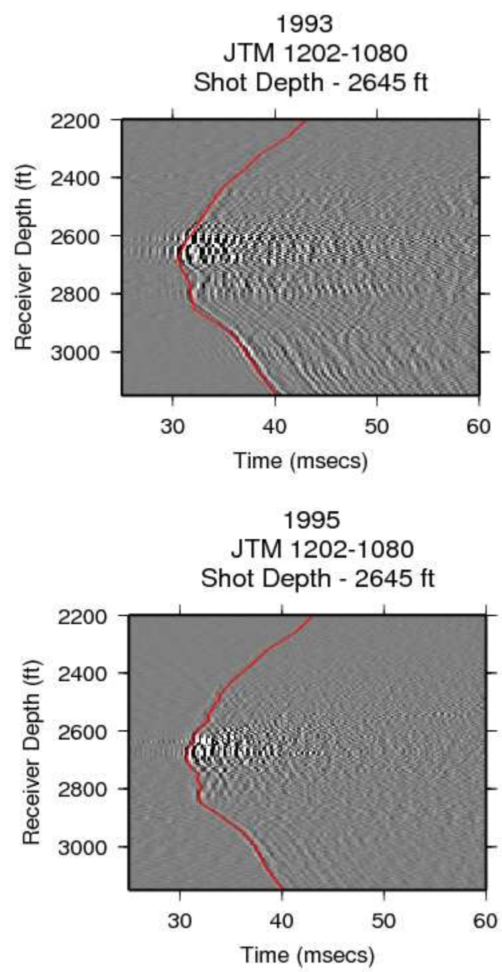


Figure 1: Common-source gathers from the 1993 and the 1995 surveys at the McElroy field in West Texas. The red lines indicated first arrivals.

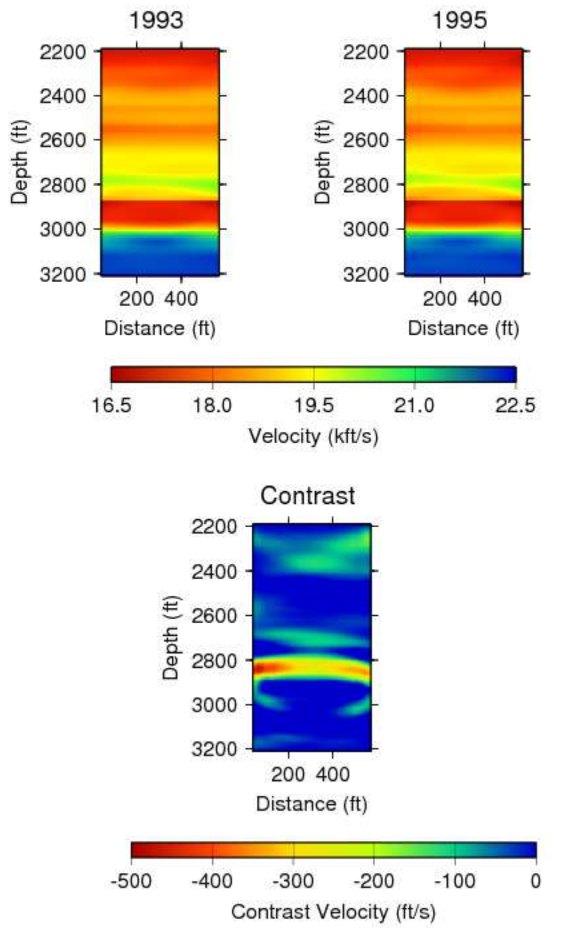


Figure 2: Reconstructed velocity models from the baseline (1993) and monitor (1995) surveys, and the difference between both models.

To test the efficiency of the approach presented in this paper on field data, we used the complete dataset from the 1993 survey and 1% of the dataset from the 1995 survey to estimate the discarded data from the 1995 dataset. Here, the **A** operator in equation (7) was the first order derivative operator. The velocity models were then reconstructed from the estimated data. Figure 3 shows the resulting contrast model. We obtained a good comparison between the true contrast model and the contrast model from the reconstructed dataset.

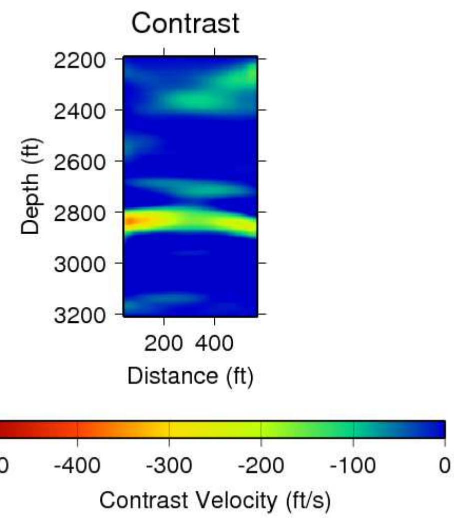


Figure 3: Reconstructed contrast model from the decimated 1995 field dataset.

**Time-lapse Synthetic Monitoring Example**

In order to test this approach of quasi-continuous monitoring, we created a series of 70 two-dimensional p-wave velocity models from the baseline model reconstructed using the 1993 dataset, and a set of simulated fluid flow models converted to velocity models. The conversion was done using a Gassmann fluid substitution model. These models are intended to simulate $CO_2$ injection into the reservoir over a period of 32 months. We included a fracture in the model which allowed injected $CO_2$ to flow out of the reservoir. Leakage occurred after the injected $CO_2$ reached the fracture zone approximately 10 months after the start of injection.

Using the finite differencing eikonal solver scheme given by Hole and Zelt (1995), we calculated dense first arrival seismic traveltimes recorded in a crosswell data acquisition geometry for all 70 synthetic velocity models. Gaussian noise with a standard deviation that we consider to be the picking error of the field data was then added to the synthetic dataset. To simulate sparse data, we reduced the data size to 10%, 5%, 2%, and 1% of the original size for a given dataset in time. The reduction was done such that the total data volume in each sampling scenario was constant. From these sparse synthesized datasets, we estimated the dense datasets using the methods described in the previous section, and then reconstructed the corresponding velocity models using traveltime tomography.

In estimating missing data, we used zeroth, first and second order derivative operators as the **A** operator in equation (7). We then used the resulting dataset to reconstruct the synthetic velocity models. We present the results of the reconstructed velocity models by their root mean square (rms) errors with respect to the known synthetic models (Figure 4). In this case, we use the rms errors measured in the regions of the model where changes are known to occur. The rms error curves of the estimated datasets show a consistent pattern. This implies that we can maintain an approximately equal level of misfit in our estimated datasets and reconstructed velocity models if we reduce data size and sample the data space more frequently in time. From the plots, we see that the rms error reduces with time, indicating the impact of additional data on data estimation. What is not captured by the rms error plots is that using only 1% data measured every two weeks, the leaked CO2 was detected soon after it occurred. With the conventional strategy such a leak might not be discovered for years.

## Conclusions

The quasi-continuous monitoring strategy presented proved effective for both synthetic and field datasets. In the synthetic example, the $CO_2$ leak which occurred in the synthetic reservoir was detected early. Even though we assumed crosswell seismic acquisition geometry, data evolution can be applied to data acquired using any kind of data acquisition geometry. We intend to continue research in the area of time-lapse seismic monitoring with sparse seismic data using full seismic traces. Future work will involve the development of techniques that will take advantage of time dependent data covariance in time-lapse data. The most challenging aspect of data evolution is deciding on the optimal data size that produces the desired results, and the optimal time-lapse survey design. The benefit of data evolution is the ability to sample the data space more frequently in time with much less data without significantly loosing spatial resolution in reconstructed velocity models. Also temporal resolution is increased with increased temporal sampling.

## Acknowledgements

We would like to thank the Global Climate and Energy Project (GCEP) for supporting this research; and the sponsors of the Seismic Tomography Project at Stanford University for providing the field dataset used and the permission to publish this work.

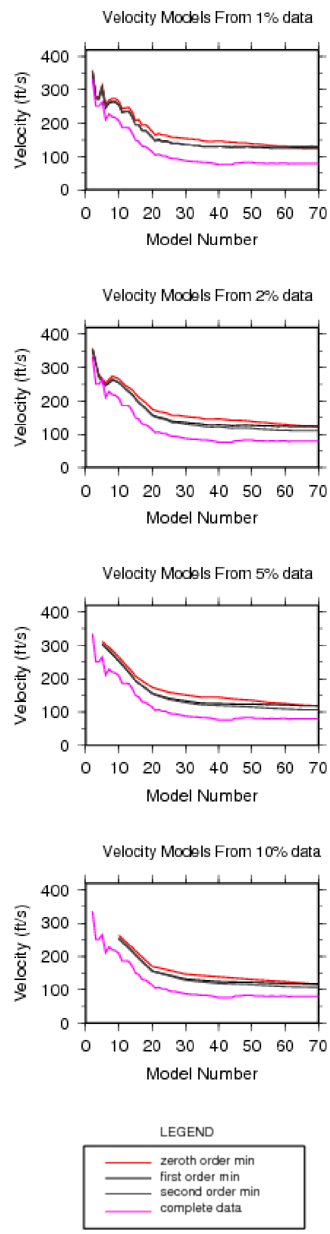


Figure 4: RMS error plots of the reconstructed velocity models using the estimated datasets.

**EDITED REFERENCES**

Note: This reference list is a copy-edited version of the reference list submitted by the author. Reference lists for the 2009 SEG Technical Program Expanded Abstracts have been copy edited so that references provided with the online metadata for each paper will achieve a high degree of linking to cited sources that appear on the Web.

**REFERENCES**

Arts, R., O. Eiken, A. Chadwick, P. Zweigel, L. van der Meer, and B. Zinszner, 2004, Monitoring of $CO_2$ injected at Sleipner using time-lapse seismic data: Energy, **29**, 1383–1392.

Candès, E., and J. Romberg, 2007, Sparsity and incoherence in compressive sampling: Inverse Problems, **23**, 969–985.

Harris, J. M., R. C. Nolen-Hoeksema, R. T. Langan, M. Van Schaack, S. K. Lazaratos, and J. W. Rector III, 1995, High resolution crosswell imaging of a west Texas carbonate reservoir: Part 1 — Project summary and interpretation: Geophysics, **60**, 667–681.

Harris, J. M., M. D. Zoback, A. R. Kovscek, F. M. Orr, Jr., 2004, Geologic storage of $CO_2$: Global Climate and Energy Project 2008 Technical Report, section 2.5.3.

———, 2007, Geologic storage of $CO_2$: Global Climate and Energy Project 2008 Technical Report, section 2.5.3.

———, 2008, Geologic storage of $CO_2$: Global Climate and Energy Project 2008 Technical Report, section 2.5.3.

Hole, J. A., and B. C. Zelt, 1995, 3-D finite-difference reflection traveltimes: Geophysical Journal International, **121**, 427–43

Lazaratos, S. K., and B. P. Marion, 1997, Crosswell seismic imaging of reservoir changes caused by $CO_2$ injection: The Leading Edge, **16**, 1300–1306.

Landrø, M., O. A. Solheim, E. Hilde, B. O. Ekren, and L. K. Strønen, 1999, The Gullfaks 4D seismic study: Petroleum Geoscience, **5**, 213–226.

Mathisen, M. E., A. A. Vasiliou, P. Cunningham, J. Shaw, J. H. Justice, and N. J. Guinzy, 1995, Time-lapse crosswell seismic tomogram interpretation: Implications for heavy oil reservoir characterization, thermal recovery process monitoring, and tomographic imaging technology: Geophysics, **60**, 631–650.

Rickett, J. E., and D. E. Lumley, 2001, Cross-equalization data processing for time-lapse seismic reservoir monitoring: A case study from the Gulf of Mexico: Geophysics, **66**, 1015–1025.

Wynn, D., 2003, Survey of geophysical monitoring methods for monitoring $CO_2$ sequestration in aquifers: M.S. thesis, Stanford University.

Yilmaz, Ö., 1987, Seismic data processing: SEG.

Yilmaz, Ö., 2001, Seismic data analysis: Processing, inversion, and interpretation of seismic: SEG.

Zelt, C. A., and P. J. Barton, 1998, 3D seismic refraction tomography: A comparison of two methods applied to data from the Faeroe Basin: Journal of Geophysical Research, **103**, 7187–7210.